Double diffusive convection in a vertical rectangular cavity

Kassem Ghorayeb, Abdelkader Mojtabi

Double diffusive convection in a vertical rectangular cavity

Kassem Ghorayeb and Abdelkader Mojtabi
U.M.R. 5502 IMFT-CNRS-UPS, U.F.R. M.I.G. 118, route de Narbonne, 31062 Toulouse Cedex, France

(Received 30 May 1996; accepted 14 April 1997)

In the present work, we study the onset of double diffusive convection in vertical enclosures with equal and opposing buoyancy forces due to horizontal thermal and concentration gradients (in the case $Gr_S/Gr_T=-1$, where Gr_S and Gr_T are, respectively, the solutal and thermal Grashof numbers). We demonstrate that the equilibrium solution is linearly stable until the parameter $Ra_T|Le-1|$ reaches a critical value, which depends on the aspect ratio of the cell, A. For the square cavity we find a critical value of $Ra_c|Le-1|=17\,174$ while previous numerical results give a value close to 6000. When A increases, the stability parameter decreases regularly to reach the value 6509, and the wave number reaches a value $k_c=2.53$, for $A\to\infty$. These theoretical results are in good agreement with our direct simulation. We numerically verify that the onset of double diffusive convection corresponds to a transcritical bifurcation point. The subcritical solutions are strong attractors, which explains that authors who have worked previously on this problem were not able to preserve the equilibrium solution beyond a particular value of the thermal Rayleigh number, Ra_{o1}. This value has been confused with the critical Rayleigh number, while it corresponds in fact to the location of the turning point.
[S1070-6631(97)01608-5]

I. INTRODUCTION

The basic feature of double diffusive convection is that two components with different rates of diffusion affect the fluid density. The origin of this field arises from oceanography[1] (heat and salt in water) but its applications are wide and include geology and crystal growth.[2–4] In the present work, we study the onset of convection in vertical enclosures with constant temperatures along the vertical sidewalls. Various convection modes exist depending on how the initial concentration gradient is imposed.

The instability of a stably stratified infinite fluid layer bounded by two rigid differentially heated vertical plates has been investigated intensively over the last three decades. As in the case of the Rayleigh–Bénard convection, a certain minimum requirement must be satisfied in order that a system of roll-cells may develop. Thorpe *et al.*[5] were the first to perform the linear stability analysis of a vertically unbounded fluid layer. They analytically predicted the onset of counter rotating pairs of rolls but experimentally observed corotating rolls. Following the original work of Thorpe *et al.*[5] several papers have dealt with this problem. All the experimental investigations concerning the sense of rotation of the rolls have confirmed the observations of Thorpe *et al.*[5] Among the more recent experimental works, we refer to Tanny and Tsinober,[6] Jeevarag and Imberger,[7] and Schladow *et al.*[8] Hart[9] and Thangam *et al.*[10] refined the analysis of Thorpe *et al.*[5] taking into account the exact boundary conditions. They obtained the full marginal stability diagram that clearly illustrates the destabilizing effect of an initially stable salinity gradient in a laterally heated slot. Their works were pursued by Hart[11] who considered the nonlinear behavior of disturbances and revealed the existence of a subcritical instability of finite amplitude. Kerr[12,13] investigated the stability of a fluid flow subjected to a vertical salinity gradient and heated from a single vertical wall. He also showed that a subcritical bifurcation is responsible for the onset of convective layers.[13]

Recently, Tsitverblit and Kit[14] and Tsitverblit[15] have numerically investigated steady-state solutions for a vertical rectangular enclosure. They show that this situation is characterized by complex steady bifurcation phenomena. Tsitverblit[15] studied the flow for several values of the salinity Rayleigh number around the borders of the double diffusive region. He reported that, when the thermal Rayleigh number is either very small or sufficiently large, the steady solution is unique, while for intermediate values of the thermal Rayleigh number, there exists a great variety of multiple steady flows.

The above works[5–15] dealt with the flow when the solutal gradient is vertical. In these works, the solutal boundary conditions on the vertical sidewalls are no-solutal flux. Another important form of the solutal boundary conditions is where the solutal gradient is horizontal instead of being vertical. The problem of the natural convection induced by buoyancy effects due to horizontal thermal and solutal gradients has received considerable attention in recent years. This situation occurs in some horizontal crystal growth techniques (e.g., horizontal Bridgman).[16] During the growth of a crystal, the profound influence of the transport process in the fluid phase on the structure and the quality of the solid phase requires a good understanding of the buoyancy convective flows in this problem. Several experimental investigations (Kamotani *et al.*,[16] Ostrach *et al.*,[17] Jiang *et al.*,[18,19] Lee *et al.*,[20] Han and Kuehn,[21] and Weaver and Viskanta[22]) and numerical investigations (Béghein *et al.*,[23] Mahajan and Angirasa,[24] Hyun and Lee,[25] Lee and Hyun,[26] Han and Kuehn,[27] Bennacer and Gobin,[28] Gobin and Bennacer,[29] and Bergman and Hyun[30]) have been reported in this field. Depending on the parameters involved, experimental observations and numerical investigations show the existence of one-cell or multicell regimes. Table I shows the range of parameters used in some

TABLE I. Range of parameters used in some of the recent papers that have been devoted to enclosures with horizontal thermal and solutal gradients.

Authors	A	Pr	Le	Gr_T	Gr_S	N
			Experimental works			
Kamotani *et al.*[16]	0.13–0.55	7	300	0–1.9×10^6	$(\mp)1.4\times10^5$–1.0×10^7	$(\mp)4$–40
Jiang *et al.*[19]	0.13–0.5	7	400–425	5.7×10^3–3.3×10^6	-1.7×10^7 to -1.1×10^5	-102 to -2.8
Lee *et al.*[20]	0.2 and 2.0	4.0–7.9	60–197	$(\mp)2.43\times10^5$–7.12×10^7	7.95×10^6–5.85×10^8	$(\mp)2.7$–72.3
Han and Kuehn[21]	1 and 4	7.8–8.8	261–333	$(\mp)1.4\times10^5$–1.1×10^6	2.7×10^6–1.8×10^7	-24–13
			Numerical works			
Han and Kuehn[11]	4	8	250	-4×10^5–3×10^5	10^5 et 3×10^6	-10–550
Béghein *et al.*[23]	1	0.71	0.5–5	1.41×10^7	-1.41×10^8 to -2.8×10^5	-0.02 to -10
Hyun and Lee[25] and Lee and Hyun[26]	2	7	100	1.97×10^3–3.94×10^7 0.28×10^6–1.97×10^7	1.97×10^7 -0.85×10^7	0.5–10000 -0.5 to -30
Bennacer and Gobin[28] and Gobin and Bennacer[29]	1 1–8	7	1–1000	10^3–10^6		0.1–100
Bergman and Hyun[30]	1	0.02	7500	5×10^3		-0.1–10

of the recent papers devoted to horizontal thermal and solutal gradients.

Given that convective flows are often undesirable in crystal growth processes,[2] the challenge is to minimize double diffusive convection in the fluid phase. In the special case where the ratio N^* of solutal to thermal Grashof numbers is equal to -1 ($N^*=Gr_S/Gr_T=-1$), the purely diffusive regime is stable up to a critical value of the thermal Rayleigh number. In this situation, the instability in the fluid is induced by the difference between solutal and thermal diffusivities. Such a situation, although difficult to produce experimentally, is an important step towards better understanding of the situation where Gr_S/Gr_T is close to -1. None of the papers mentioned so far[16–30] have considered the situation where $N^*=-1$ (Table I). However, two recent papers were devoted to this situation. Krichnan[31] numerically studied the transition from the purely diffusive regime to the steady convective regime and time-dependent regimes in the case of a square cavity. The numerical study indicates that the onset of convection occurs at a critical Rayleigh number $Ra_c=3000$ $[Ra_c(Le-1)=6481]$ a limit below which the purely diffusive steady-state solution is stable. Gobin and Bennacer[32] studied the onset of double diffusive natural convection. Their analytical study concerned an infinite vertical layer with impermeable and slip boundary conditions. The analytical solution they proposed for the linearized system corresponds to that used by Thorpe *et al.*[5] for the case of an initially stratified vertical layer of fluid. They showed that the critical Rayleigh number and the Lewis number satisfy the relation: $Ra_c(Le-1)=6122$ for an infinite vertical layer with slip boundary conditions. It is reported that an aspect ratio $A=2$ minimizes the critical Rayleigh number, a result which differs from our theoretical and numerical observations. In the present work we establish that the stability parameter $Ra_c(Le-1)$ decreases with the aspect ratio.

The main goal of the present work is to study the linear stability of the motionless solution in a vertical enclosure with constant temperatures and concentrations on the vertical sidewalls. Our interest will be focused on the case where $N^*=-1$. The linear stability analysis is developed for both the case of an infinite vertical layer and the case of a vertical rectangular enclosure. We plot the marginal stability diagram showing the dimensionless stability parameter $Ra_c|Le-1|$ versus the aspect ratio of the enclosure. We also performed direct numerical investigations near the onset of double diffusive convection that we compare to the analytical results. The numerical investigations were carried out for Lewis numbers varying between 2 and 151 for the aspect ratios 1, 2, 4, and 7. The Prandtl number is fixed at the value 1. The thermal Grashof number values considered in the numerical study satisfy $0<Gr_T(Le-1)\leqslant 3\times10^4$.

II. MATHEMATICAL FORMULATION

The system of equations is assumed to be unsteady state with no heat generation, viscous dissipation, chemical reactions, or thermal radiation. The Oberbeck–Boussinesq approximation is assumed to be valid, thermophysical properties are constant except in the buoyancy term where

$$\rho(T,C)=\rho_0(1-\beta_T(T-T_0)-\beta_C(C-C_0)).$$

Here $\rho_0=\rho(T_0,C_0)$, $\beta_T=(-1/\rho_0)(\partial\rho/\partial T)_C$, and $\beta_C=(-1/\rho_0)(\partial\rho/\partial C)_T$ are, respectively, the density at temperature T_0 and concentration C_0, the thermal expansion coefficient, and the solutal expansion coefficient. The conservation equations for momentum, mass, energy, and species in dimensionless form are

$$\frac{\partial\mathbf{U}}{\partial t}+(\mathbf{U}\cdot\nabla)\mathbf{U}=-\nabla P+\nabla^2\mathbf{U}+(Gr_T T+Gr_S C)\mathbf{k}, \tag{1}$$

$$\nabla\cdot\mathbf{U}=0, \tag{2}$$

$$\frac{\partial T}{\partial t}+\mathbf{U}\cdot\nabla T=\frac{1}{Pr}\nabla^2 T, \tag{3}$$

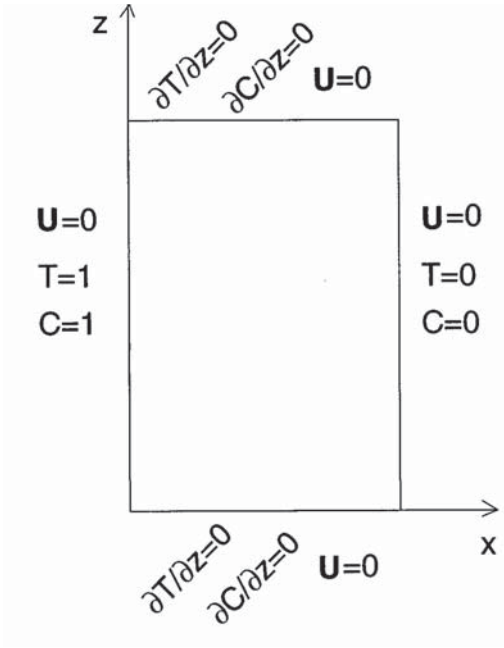

FIG. 1. The geometry of a vertical rectangular enclosure showing the boundary conditions.

$$\frac{\partial C}{\partial t}+\mathbf{U}\cdot\nabla C=\frac{1}{Sc}\nabla^2 C, \tag{4}$$

where $Gr_T=(g\beta_T\Delta TL^3)/\nu^2$ is the thermal Grashof number, $Gr_S=(g\beta_C\Delta CL^3)/\nu^2$ the solutal Grashof number, $Pr=\nu/\chi$ the Prandtl number, and $Sc=\nu/D$ the Schmidt number. D, χ, ν, and g, are the solutal diffusivity, the thermal diffusivity, the kinematic viscosity, and the gravity acceleration, respectively. The corresponding boundary conditions (Fig. 1) are

$$\mathbf{U}=0(x=0,\ x=1,\forall z \quad \text{and} \quad z=0,\ z=A,\forall x), \tag{5}$$

$$T=C=1 \quad (x=0,\forall z), \tag{6}$$

$$T=C=0 \quad (x=1,\forall z), \tag{7}$$

$$\frac{\partial T}{\partial z}=\frac{\partial C}{\partial z}=0 \quad (z=0,\ z=A,\forall x). \tag{8}$$

In the above equations, lengths are nondimensionalized by L, velocity by ν/L, time by L^2/ν, temperature by $\delta T=T_2-T_1$, and concentration by $\delta C=C_2-C_1$. T_1, C_1, T_2, and C_2 are the temperature and the concentration at $x=0$ and $x=L$, respectively. We assume that $\beta_T>0$ and $\beta_C<0$ (ρ increases with C and decreases with T) and that $T1>T2$ and $C1>C2$. This assumption leads to $Gr_T>0$ and $Gr_S<0$. The buoyancy ratio $N^*=Gr_S/Gr_T$ is fixed at the value -1.

III. LINEAR STABILITY

We study the linear stability of the equilibrium solution $\mathbf{U}_0=0$, $T_0=1-x$, and $C_0=1-x$ obtained for $Gr_S/Gr_T=-1$. We denote (ψ, θ, c) the perturbation quantities for the stream function, temperature, and concentration. If we assume that the principle of exchange of stability is valid, we obtain the following linearized system of equations:

$$\Delta^2\psi+Gr_T\left(\frac{\partial c}{\partial x}-\frac{\partial\theta}{\partial x}\right)=0, \tag{9}$$

$$\frac{\Delta\theta}{Pr}+\frac{\partial\psi}{\partial z}=0, \tag{10}$$

$$\frac{\Delta c}{Sc}+\frac{\partial\psi}{\partial z}=0, \tag{11}$$

with the following boundary conditions:

$$\frac{\partial c}{\partial z}=\frac{\partial\theta}{\partial z}=\frac{\partial\psi}{\partial x}=\frac{\partial\psi}{\partial z}=0(z=0,\ z=A,\forall x), \tag{12}$$

$$c=\theta=\frac{\partial\psi}{\partial x}=\frac{\partial\psi}{\partial z}=0(x=0,\ x=1,\forall z). \tag{13}$$

Equations (10) and (11) together with the boundary conditions (12) and (13) imply

$$c=Le\,\theta, \tag{14}$$

where $Le=Sc/Pr$ is the Lewis number. This result shows that, near the bifurcation point, the perturbed parts of the temperature and the concentration are similar, a result which is in a good agreement with our numerical simulations.

Eliminating c in the system of equations (9) and (11), we obtain a fourth-order system of equations governing the variables θ and ψ:

$$\Delta^2\psi+Gr_T(Le-1)\frac{\partial\theta}{\partial x}=0, \tag{15}$$

$$\frac{\Delta\theta}{Pr}+\frac{\partial\psi}{\partial z}=0. \tag{16}$$

We notice, by replacing ψ with $Pr\psi$ in Eqs. (15) and (16) that, the linear stability parameter is $Ra_T(Le-1)$ ($Ra_T=PrGr_T$).

The condition for a nonzero solution for the system (15) and (16) leads to $Ra_c(Le-1)=\pm f(A)$ with $f(A)>0$. This last relation becomes $Ra_c(Le-1)=f(A)$ and $Ra_c(Le-1)=-f(A)$ for $Le>1$ and $0<Le<1$, respectively. In the following, $Ra_c(Le-1)$ is replaced by $Ra_c|Le-1|$.

A. Infinite vertical layer

We consider an infinite vertical layer. Our attention is focused on the value of the critical Rayleigh number, corresponding to the onset of convection. This situation has been studied by Gobin and Bennacer[32] following the analysis carried out by Thorpe *et al.*[5] The analytical solution they used only satisfies the impermeability condition at the boundary planes. They have reported that the critical Rayleigh number and the Lewis number are related by $Ra_T|Le-1|=6122$.

We study the same situation in this section. Equations (15) and (16), with all the boundary conditions along the vertical walls, are solved with both the Galerkin method and the compound matrix method.

TABLE II. Infinite vertical layer: results obtained for $Ra_c|Le-1|$ and k_c for several orders of truncation of series.

N	k_c	$Ra_c\|Le-1\|$
2	2.48	7230
3	2.52	6892
4	2.53	6622
5	2.53	6620

1. The Galerkin method

The Galerkin method has been used in several works concerning convective instability problems. The linear stability of a fluid contained in a vertical slot has been studied using this method by Hart[9] and Thangam *et al.*[10] The success of this method in these two investigations motivated its use in the present problem of double diffusive convection in a vertical fluid layer. The perturbation functions used here are

$$\psi=\sum_{n=1}^{N} a_n \sin(\pi x)\sin(n\pi x)e^{Ikz}, \tag{17}$$

$$\theta=\sum_{n=1}^{N} b_n \sin(n\pi x)e^{Ikz}, \tag{18}$$

where k is the wave number and I is the pure imaginary number ($\sqrt{-1}$). The trial functions for ψ verify: $\mathbf{U}=0$ for $x=0,1$ whereas in the previous work of Gobin and Bennacer[32] only the condition $\mathbf{U}\cdot\mathbf{x}=0$ for $x=0,1$ is satisfied. The results show that, with only five terms in the truncated series, convergence occurs. The results for $N=4$ differ by less than 0.1% from those for $N=5$ (Table II). This approach, based on the Galerkin method, gives the following value for the dimensionless group: $Ra_c|Le-1|=6620$ which corresponds to the critical wave number $k_c=2.53$. The mathematical complexity of the problem when N increases led us to use another approach (the compound matrix method) in order to obtain more accurate results for the critical stability parameters.

2. The compound matrix method

Equations (15) and (16) lead to

$$\Delta^3\theta+Ra_T(Le-1)\frac{\partial^2\theta}{\partial x\,\partial z}=0. \tag{19}$$

Using the equations (15) and (16) and the boundary conditions (12) and (13), we obtain the six boundary conditions which are necessary to solve the sixth-order partial differential equation (19):

$$\theta=\frac{\partial^2\theta}{\partial x^2}=\frac{\partial^3\theta}{\partial x^3}+\frac{\partial^3\theta}{\partial x\,\partial z^2}=0(x=0,1,\forall z). \tag{20}$$

Assuming that

$$\theta=e^{Ikz}\,\overline{\theta}(x), \tag{21}$$

Eqs. (19) and (21) imply that

$$\left[\frac{d^2}{dx^2}-k^2\right]^3\overline{\theta}-Ra_T(Le-1)Ik\frac{d\,\overline{\theta}}{dx}=0. \tag{22}$$

The corresponding boundary conditions are

$$\overline{\theta}=\overline{\theta''}=\overline{\theta'''}-k^2\,\overline{\theta'}=0(x=0,1,\forall z), \tag{23}$$

where $\overline{\theta'}=d\,\overline{\theta}/dx$, $\overline{\theta''}=d^2\,\overline{\theta}/dx^2$, etc.

We used the compound matrix method to solve Eq. (22) with boundary conditions (23). A very clear description of this method and its applications in hydrodynamic stability problems is given by Drazin and Reid.[33] Here, we show how this method is used to find the critical Rayleigh number corresponding to the lowest eigenvalue of (22). To solve the problem (22) and (23) by this method, we let $\overline{\Theta}=(\overline{\theta},\overline{\theta'},\overline{\theta''},\overline{\theta'''},\overline{\theta^{(4)}},\overline{\theta^{(5)}})^T$. To determine the lowest eigenvalue, we retain the three conditions at $x=0$. The boundary conditions at $x=1$ on $\overline{\theta}$, $\overline{\theta''}$, and $\overline{\theta'''}-k^2\,\overline{\theta'}$ are replaced in turn by ($\overline{\theta'}=1$, $\overline{\theta^{(4)}}=0$, $\overline{\theta^{(5)}}=0$), ($\overline{\theta'}=0$, $\overline{\theta^{(4)}}=1$, $\overline{\theta^{(5)}}=0$), and then ($\overline{\theta'}=0$, $\overline{\theta^{(4)}}=0$, $\overline{\theta^{(5)}}=1$), at $x=0$. The boundary value problem is thus converted into an initial value problem. Let the solution so found be written as a linear combination of the three solutions so obtained, say, $\overline{\Theta}=\alpha_1\overline{\Theta}_1+\alpha_2\overline{\Theta}_2+\alpha_3\overline{\Theta}_3$, where $\overline{\Theta}_1$, $\overline{\Theta}_2$, and $\overline{\Theta}_3$ are solutions of (22) with values at $x=0$: $(0,1,0,k^2,0,1)^T$, $(0,0,0,0,1,0)^T$, and $(0,0,0,0,0,1)^T$, respectively. α_1, α_2, and α_3 are constants. A new 20 element vector $Y=(y_1,\ldots,y_{20})^T$ is defined as the 3×3 minors of the 6×3 solution matrix whose first column is $\overline{\Theta}_1$, second $\overline{\Theta}_2$, and third $\overline{\Theta}_3$. By direct calculation from (22), we obtain an initial value problem for Y:

$$Y'=L(Y), \tag{24}$$

where L is a linear operator.

Problem (24) together with the conditions obtained from the initial conditions on $\overline{\Theta}_1$, $\overline{\Theta}_2$, and $\overline{\Theta}_3$, is solved using a fourth-order Runge–Kutta technique. The results obtained for both the critical Rayleigh number and the critical wave number are

$$Ra_c|Le-1|=6509$$

and

$$k_c=2.53.$$

B. Vertical enclosure

In their investigations on the influence of the aspect ratio on the critical Rayleigh number, Gobin and Bennacer[32] reported that the critical Rayleigh number obtained numerically for a closed cavity with no-slip boundary conditions, for all values of $A>1$, is below the analytical value obtained for an infinite vertical layer. Here we present a more complete analysis of the stability of the pure diffusive solution for a vertical enclosure with boundary conditions (5)–(8). As in the case of the infinite vertical layer, the Galerkin method is used. The perturbation functions used are

$$\psi=\sum_{n=1}^{N}\sum_{m=1}^{M} a_{nm}\psi_{nm}, \tag{25}$$

$$\theta=\sum_{n=1}^{N}\sum_{m=1}^{M} b_{nm}\theta_{nm}, \tag{26}$$

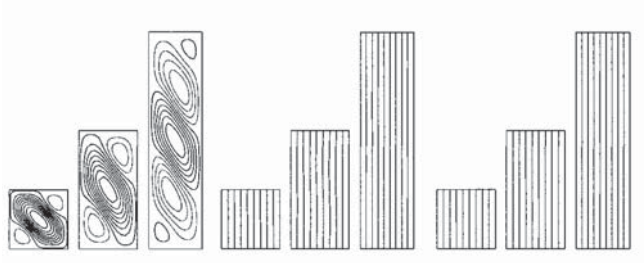

FIG. 2. The supercritical solution for $A=1$, $A=2$, and $A=4$ corresponding to $Ra_T=1750$, $Ra_T=900$, and $Ra_T=700$, respectively.

where the trial functions ψ_{nm} and θ_{nm} are

$$\psi_{nm}=\sin(\pi x)\sin(n\pi x)\sin\left(\pi\frac{z}{A}\right)\sin\left(m\pi\frac{z}{A}\right),$$

and

$$\theta_{nm}=\sin(n\pi x)\cos\left(m\pi\frac{z}{A}\right),$$

in which it can be seen easily that the trial functions ψ_{nm} and θ_{nm} verify all the conditions (12) and (13). The order of truncation of the series ($N=14$, $M=14$) is sufficient for convergence in the case of a square cavity. The difference between the results for the approximations ($N=14$, $M=14$) and ($N=16$, $M=16$) is less than 0.1%. The value of the critical Rayleigh number obtained with the approximation ($N=14$, $M=14$) is $Ra_c|Le-1|=17\,198$. However, the case of a square cavity was investigated up to the order ($N=22$, $M=22$) so as to find a value for $Ra_c|Le-1|$ with high accuracy. This approximation leads a value of $Ra_c|Le-1|$ of 17 174. This value differs by less than 0.15% and 0.01% from that obtained for ($N=14$, $M=14$) and ($N=20$, $M=20$), respectively. It is therefore assumed that convergence occurs for ($N=14$, $M=14$). It is noted that, even at ($N=8$, $M=8$), the value obtained for $Ra_c|Le-1|$ is within 0.6% of that obtained with ($N=14$, $M=14$).

In order to maintain the accuracy of the results, different truncations of series have to be used depending on the aspect ratio A. It is assumed that the ratio M/N must be close to A. Such an assumption is deemed to be essential in view of the numerical results obtained. In fact, the numerical results show that the cell number increases with A. For example, in the case $A=4$, there are three big cells and two other smaller cells. However, for $A=1$, the supercritical solution is characterized by only one big cell and two other smaller cells (Fig. 2). We investigate the problem up to the following orders of truncation: ($N=14$, $M=28$), ($N=14$, $M=32$), ($N=14$, $M=56$), ($N=10$, $M=50$), ($N=10$, $M=70$), and ($N=8$, $M=80$) for $A=2$, $A=3$, $A=4$, $A=5$, $A=7$, and $A=10$, respectively (Table III). It can be shown that the critical Rayleigh number obtained for $A=7$ differs by less than 0.5% from the one obtained for $A=10$. This means that the critical Rayleigh number converges, when A increases, to the value obtained for an infinite vertical layer: $Ra_c|Le-1|=6509$ (Fig. 3). Results show that, for all aspect ratios, the value of the critical Rayleigh number is greater than the value of the critical Rayleigh number obtained for the case of an infinite vertical layer (Fig. 3). These results will be confirmed numerically in the following section.

TABLE III. Enclosures: results obtained for $Ra_c|Le-1|$ for several orders of truncation of series. $M=A\times N$.

$N\backslash A$	1	2	3	4	5	7	10
6	17 426	8774	7427	7044	6947	6789	6637
8	17 299	8739	7399	7018	6854	6698	6614
10	17 243	8724	7387	7007	6844	6688	
12	17 214	8716	7381	7002			
14	17 198	8710	7377	6998			
16	17 188	8709	7375				
18	17 182						
20	17 176						
22	17 174						

IV. NUMERICAL RESULTS

A. Numerical scheme

The numerical method used here is based on the projection diffusion algorithm developed by Batoul *et al.*[34] for solving two-dimensional unsteady incompressible Navier–Stokes equations. The temporal integration consists of a semi-implicit second-order finite differences approximation. The linear (viscous) terms are treated implicitly by the second-order Euler backward scheme, while a second-order explicit Adams–Bashforth scheme is used to approximate the nonlinear (advective) parts. A high-accuracy spectral method, namely, the Chebyshev collocation method, with the Gauss–Lobatto zeros as collocation points, is used for the spatial discretization (Khallouf[35]).

B. Results and discussion

Figure 4 summarizes the terminology which was used in this section: transcritical bifurcation point, turning point, equilibrium regime (solution), supercritical regime (solution)

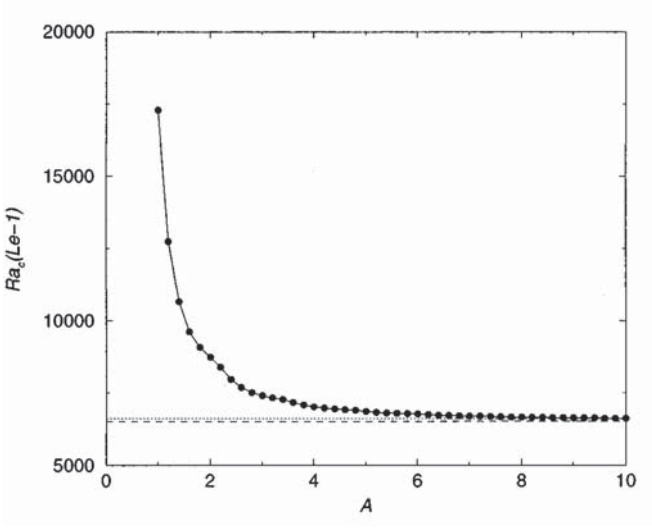

FIG. 3. Results obtained by the linear stability analysis for enclosures (circles) and for the infinite layer both by the Galerkin method (dotted line) and the compound matrix method (dashed line).

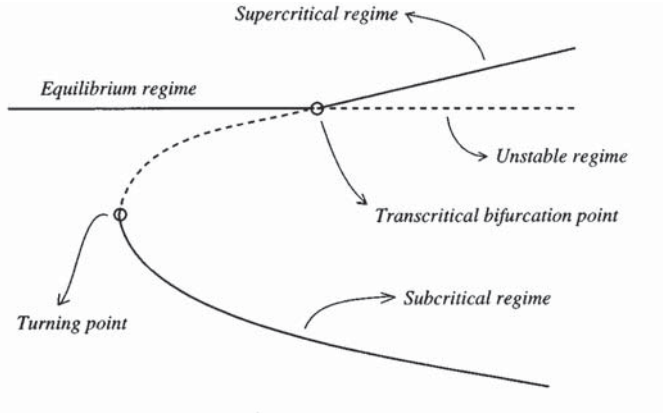

FIG. 4. Stability terminology used in the text. The solid and dashed lines designate stable and unstable branches of solution.

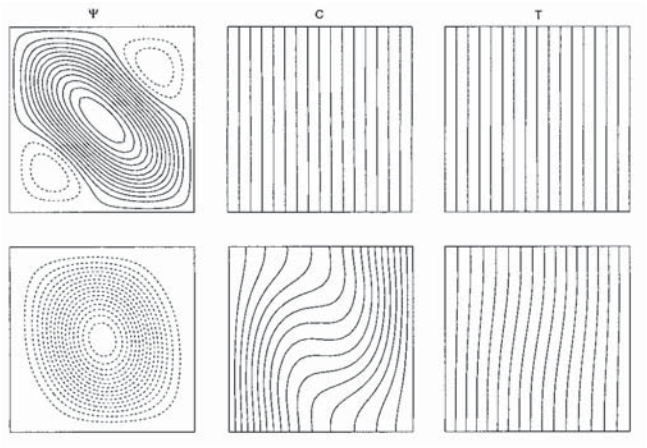

FIG. 5. Square cavity: supercritical (top) and subcritical (bottom) regimes corresponding to $Ra_T=1750$ and $Ra_T=680$, respectively, $Le=11$. The dashed and solid lines designate the clockwise and the counterclockwise rotations, respectively.

and subcritical regime (solution). This section will be restricted to values of the Lewis number larger than 1 which correspond to a thermal diffusivity larger than the solutal one.

The disagreement between the results obtained by our linear stability analysis for an enclosure and those found numerically by Krichnan[31] and Gobin and Bennacer[32] led us to undertake this numerical study. In fact, in their studies, Krichnan[31] and Gobin and Bennacer[32] have obtained, for a square cavity, a value of $Ra_c(Le-1)$ close to 6000. This value differs greatly from that found by the Galerkin method (17 174). The numerical study that we undertook produces a value for $Ra_c(Le-1)$ which is very close to that obtained by our linear stability analysis. The values of $Ra_c(Le-1)$ obtained numerically differ by less than 0.1% from those obtained by linear stability analysis, for all values of the aspect ratio which were studied.

For a square cavity, two convective regimes were observed. The purely diffusive regime forks to the supercritical regime at the value $Ra_c|Le-1|=17\,161$ (or $Ra_c|Le-1|=17\,174$ according to linear stability analysis). The supercritical regime is a three-cell one (Fig. 5). The principal (central) cell rotates counterclockwise. The two other cells, induced by the principal cell rotate clockwise. They are symmetric to each other with respect to the center of the cavity (Fig. 5). Their intensity is very small compared with that of the principal cell. A physical illustration of the sense of rotation of the three cells is now developed.

Let us consider two fluid particles p_1 and p_2 each of which being near the middle of a vertical sidewall, in a purely diffusive state corresponding to $Ra_T=Ra_c+\epsilon^2$ ($\epsilon^2 \ll Ra_c$). Suppose now that each of these particles is slowly and infinitesimally displaced away from the vertical side. The particle p_1 near the warmer and higher concentration wall (left wall, $x=0$) will be cooled but its salinity will not change very much, owing to a smaller value of the solutal diffusivity ($Le>1$). Thus particle p_1 becomes denser than its surroundings and moves downward with very low velocity toward the bottom. This downward motion continues until the particle density reaches the density of its surroundings (because of thermal gain). The downward motion of particle p_1 is then decelerated and it is deflected away from the (left) wall because the temperature away from the (left) wall is less than that of particle p_1. In addition, due to viscous effects, this motion generates a clockwise rotating cell in the left bottom corner. The size of this cell depends on the values of the thermal Rayleigh number and the Lewis number. Particle p_2 near the colder and low concentration side (right wall, $x=1$) moves up.

The subcritical regime occurs for lower thermal Rayleigh numbers. For a Lewis number $Le=11$, for example, this regime occurs for values of thermal Rayleigh number larger than $Ra_{o1}=676$, which is nearly three times smaller than the critical Rayleigh number ($Ra_c=1716.1$). The subcritical solution is a single clockwise rotating cell (Fig. 5). The simplest physical explanation of the direction of rotation of this cell has been reported by Thorpe *et al.*[5] in a similar case. Let us consider two fluid particles lying at the same horizontal level in a fluid only containing horizontal thermal and solutal gradients which balance each other such that the resulting density gradient vanishes. If the particles of fluid are interchanged (finite disturbances), the particle introduced into warmer and more concentrated surroundings becomes warmer but not very concentrated, since the thermal diffusivity is greater than the solutal one ($Le>1$), and therefore rises, being less dense than its concentration surroundings, while the other particle sinks. Thus we generated a clockwise rotating cell. This physical argument ignores the viscosity which plays its part in providing a criterion for the onset of convection.

However, our numerical investigations showed that the onset of double diffusive convection corresponds to a transcritical bifurcation point. Thus the values of the thermal Rayleigh number obtained by Krichnan[31] and Gobin and Bennacer[32] for the onset of double diffusive convection correspond to the location of a turning point Ra_{o1}. Indeed, when we gradually increase the thermal Rayleigh number starting from the equilibrium solution, we observe that the solution switches rapidly to the convective regime at the value obtained by Krichnan[31] and Gobin and Bennacer[32] and identi-

fied by them as the critical Rayleigh number. In order to remain on the equilibrium solution for Rayleigh numbers higher than the values given by Krichnan[31] and Gobin and Bennacer,[32] it would be necessary to proceed cautiously with the numerical solution since the subcritical solution is a stronger attractor than the equilibrium solution.

These results are similar to those obtained by the weakly nonlinear analysis reported by Hart[11] and Kerr[13] for the case of a stably stratified vertical layer of fluid subjected to lateral heating. They showed that the bifurcation from stability was subcritical for the large range of parameters, and so the form of the observed instabilities would not necessarily be similar to the form of the linear disturbances predicted at marginal stability.

The linear stability analysis and relevant numerical simulations show, for cavities with large aspect ratios, a flow with counterrotating convection cells. This is in good agreement with the results obtained by the linear stability analysis reported by Thorpe *et al.*,[5] Hart,[9] and Kerr.[12]

Numerical results show, for cavities with large aspect ratio, that the first instability in the fluid leads to a flow where the convection cells circulate in the same direction. This result is similar to the experimental observations of Tanny and Tsinober[6] and were also predicted by the weakly nonlinear analysis reported by Kerr.[13]

The numerical study, furthermore, shows a multiplicity of subcritical solutions, whose number increases as the aspect ratio increases. To describe these multiple flows and their stability, we are currently developing a continuation method. For the present work, we only mention that this problem has a great multiplicity of subcritical solutions depending on the aspect ratio of the cavity. In the following section, we develop a study on the influence of the Lewis number and the aspect ratio on the behavior of the supercritical regime in a region of Ra_T close to the critical Rayleigh number. The influence of the Lewis number on the subcritical regime will be studied only for the square cavity.

1. Influence of the Lewis number

In order to investigate the influence of the Lewis number on both the supercritical solutions and subcritical regimes, we selected several values of the Lewis number over the interval [2-151]. The values studied were $Le=2$, $Le=4$, $Le=7$, $Le=11$, $Le=21$, $Le=41$, $Le=61$, $Le=81$, $Le=101$, $Le=125$, and $Le=151$. It should be noted that the convergence is very slow when $Le\rightarrow 1$. Thus, our numerical investigations have been restricted to the values of $Le\geqslant 2$.

Near the purely diffusive solution, the numerical computations confirm the results obtained by the linear stability analysis. The dimensionless group $Ra_c(Le-1)$ is constant for all values of Le used. We studied the flow for a cavity with aspect ratios of $A=1$, $A=2$, and $A=4$. The results obtained for those values of aspect ratio were $Ra_c(Le-1)=17\,161$, $Ra_c(Le-1)=8700$ and $Ra_c(Le-1)=6992$ respectively. In comparison, the linear stability analysis yields: $Ra_c(Le-1)=17\,174$ for $A=1$, $Ra_c(Le-1)=8709$ for $A=2$, and $Ra_c(Le-1)=6998$ for $A=4$. The difference between the numerical results and those obtained by the linear stability analysis is less than 0.1%. Figure 6 shows this result in the case of a square cavity.

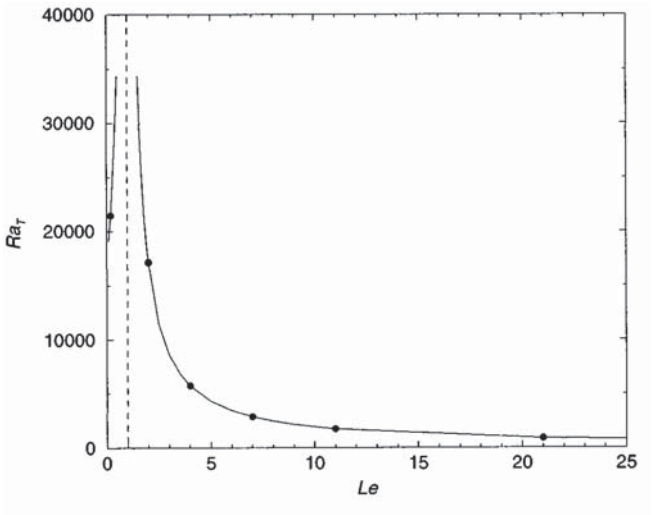

FIG. 6. Comparison between the values of the critical Rayleigh number obtained by the linear stability analysis (solid line) and those which have been obtained numerically (circles). The figure shows the critical Rayleigh number as function of the Lewis number for a square cavity.

With regard to the influence of the Lewis number on the subcritical solutions, numerical results show that, qualitatively, we obtain the same flow regimes for all values of Lewis number used. For the square cavity we find that $Ra_{o1}Le$ decreases asymptotically when Le increases. For large values of the Lewis number, Ra_{o1} reaches the value 7200. Figure 7 shows the behavior of $Ra_{o1}Le$ as a function of Le. The difference between the value of $Ra_{o1}Le$ obtained for $Le=101$ and for $Le=81$ is less than 0.15%, while a considerable variation of $Ra_{o1}Le$ occurs in the region $Le<21$ (Fig. 7). On a log-log graph, Ra_{o1} decreases linearly with Le for $Le>21$. The slope of this linear curve is equal to -1.

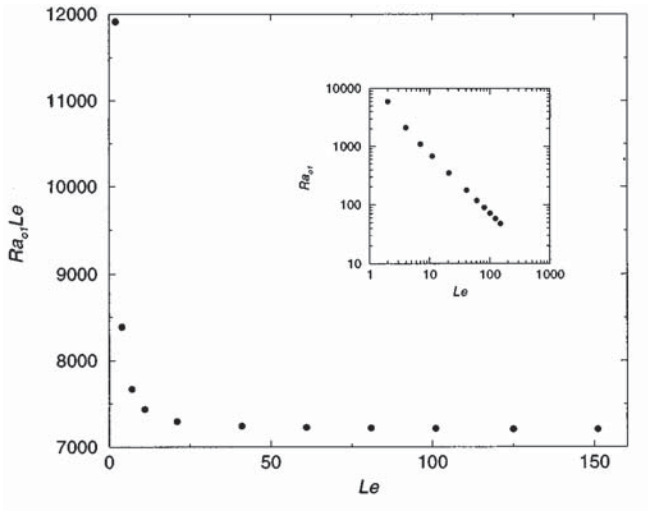

FIG. 7. Behavior of the values of the thermal Rayleigh number corresponding to the onset of the subcritical regime for a square cavity as a function of the Lewis number.

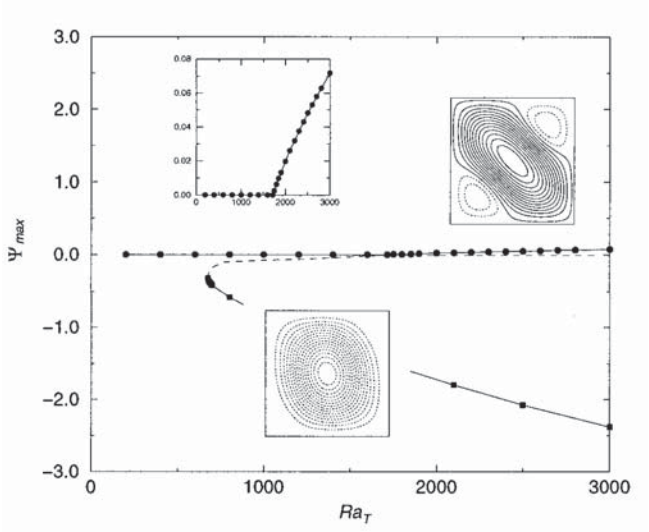

FIG. 8. Behavior of the extremum value of the dimensionless stream function as a function of the Rayleigh number for a square cavity, for both the supercritical regime (circles) and the subcritical regime (squares). The zoom shows the supercritical regime in more detail. The dashed branch designates predictive mapping of the unstable solution branch.

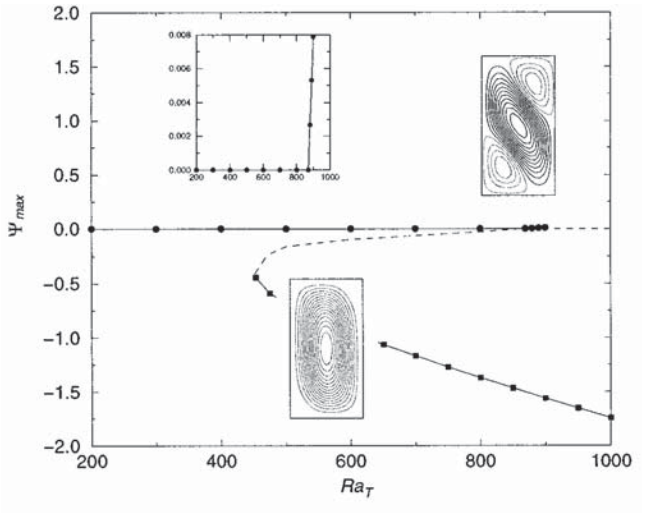

FIG. 9. Behavior of the extremum value of the dimensionless stream function as a function of the Rayleigh number for a cavity with aspect ratio $A=2$, for both the supercritical regime (circles) and the subcritical regime (squares). The zoom shows the supercritical regime in more detail. The dashed branch designates predictive mapping of the unstable solution branch.

2. Influence of the aspect ratio

In view of the ''qualitative'' independence of the flow characteristics with respect to the Lewis number, the study was restricted to the case of $Le=11$. This value of the Lewis number will be used for all following investigations. The aspect ratio used varies between 1 and 15.

a. Supercritical regime. The supercritical regime can be considered as a quasi-static one (Fig. 2). The corresponding isotherms and isoconcentration lines look like the ones obtained for the purely diffusive regime. For the case of a square cavity, the extremum value for the stream function is less than 0.1 in all the intervals of the thermal Rayleigh number for which this solution exists (Fig. 8). We notice that (Figs. 8 and 9), the extremum value of the stream function $\Psi_{\max}$ varies linearly with Ra_T in the vicinity of Ra_c ($Ra_T \geqslant Ra_c$). We also notice that the Nusselt number varies quadratically over this range of Rayleigh numbers (Figs. 10 and 11). Thus the linear variation of $\Psi_{\max}$ according to Ra_T allows us to determine by extrapolation, with great accuracy, the value of the critical Rayleigh number. For $A=1$, the slope P of the linear curve $\Psi_{\max}(Ra_T)$: $d\Psi_{\max}(Ra_T)/dRa_T$ is equal to $P=0.073\times10^{-3}$. This slope increases with A and becomes $P=0.260\times10^{-3}$ for $A=2$. For $A=4$, the value of this slope is $P=2.02\times10^{-3}$. It should be mentioned that, for large aspect ratios, it is difficult to obtain the supercritical regime. In the case of $A=1$, the supercritical solution can be obtained only in the interval [1715-3000] for Ra_T. This interval becomes [880-900] and [699-701] for $A=2$ and $A=4$, respectively. For an aspect ratio of $A=7$, for example, the convergence is largely related to the initial conditions. In the case of $A=7$, convergence of the supercritical solution was not obtained.

b. Subcritical regimes. Equations (1)–(4) together with boundary conditions (5)–(8) are symmetric with respect to the following symmetry operator:

$$L_1\begin{pmatrix}\mathbf{U}\\ T\\ C\end{pmatrix}=\begin{pmatrix}-\mathbf{U}(1-x,1-z)\\ 1-T(1-x,1-z)\\ 1-C(1-x,1-z)\end{pmatrix}.$$

Over the interval $1<A<2.5$, there is a unique subcritical solution, which is the single clockwise rotating cell flow solution. For an aspect ratio of $A>2.5$, multiple steady convective solutions were observed, for $Ra_T<Ra_c$, depending on the initial conditions used in the numerical investigations.

In the case of a cavity with an aspect ratio of $A=4$, for example, three steady solution types were obtained, two of

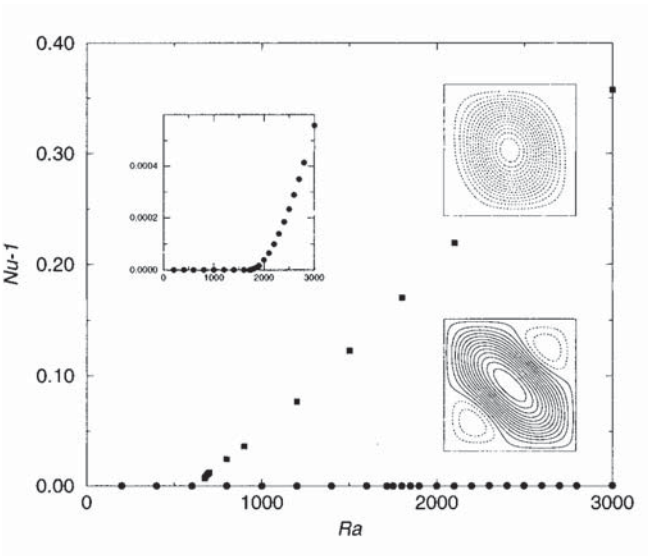

FIG. 10. Behavior of the Nusselt number as a function of the Rayleigh number for a square cavity for both the supercritical regime (circles) and the subcritical regime (squares). The zoom shows the supercritical regime in more detail.

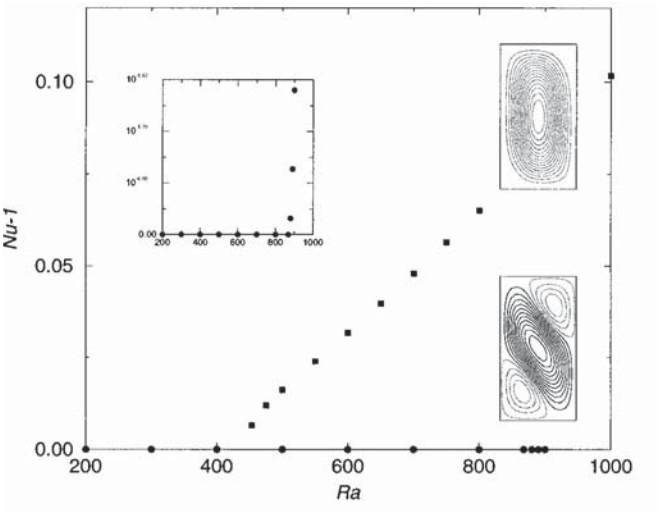

FIG. 11. Behavior of the Nusselt number as a function of the Rayleigh number for a cavity with an aspect ratio $A=2$, for both the supercritical regime (circles) and the subcritical regime (squares). The zoom shows the supercritical regime in more detail.

them presenting central symmetry and one being asymmetric (Fig. 12). Four steady solution types were obtained for the cavity with an aspect ratio $A=7$, two presented central symmetry, while the two others were asymmetric (Fig. 13).

It should be mentioned that the first subcritical instability in the fluid is of type 3 (Figs. 12 and 13) where there are two convection cells circulating in the same direction. This result is similar to that observed experimentally[6] and predicted theoretically[13] for the case of a stably stratified layer of fluid differentially heated from its vertical side walls.

V. CONCLUSION

Theoretical calculations and numerical simulations of double diffusive convection in a rectangular cavity, with equal and opposing buoyancy forces due to horizontal thermal and concentration gradients, were carried out in the case $2 \leqslant Le \leqslant 151$, for several values of the aspect ratio. The linear stability analysis developed in this work, for both an infinite vertical layer and a rectangular cavity, shows that the physical problem has only one nondimensional linear stability parameter $Ra_c(Le-1)$. The thermal Rayleigh number domain corresponding to the beginning of convective flow was investigated. The dimensionless group $Ra_c(Le-1)$ obtained by the linear stability analysis, for the square cavity, is three times higher than that given by earlier authors. Our stability analysis results are compared, for many values of aspect ratio and Lewis number, to the critical values determined from direct simulations based on a spectral method. A very good agreement between analytical and numerical results was obtained.

Numerical results show the existence of a great variety of subcritical regimes. Their number depends on the aspect ratio A of the enclosure. For the square cavity, there is a unique subcritical regime. The value Ra_{o1} of the thermal Rayleigh number, threshold of the subcritical regime, was shown to be a turning point location. Numerical investiga-

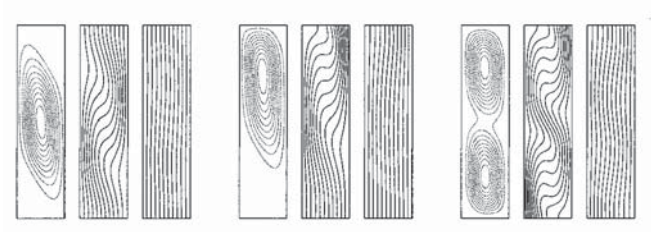

FIG. 12. The multiplicity of subcritical solutions for a cavity with an aspect ratio of $A=4$, all the three solutions correspond to $Le=11$, $Ra_T=550$. The dotted lines designate clockwise rotation.

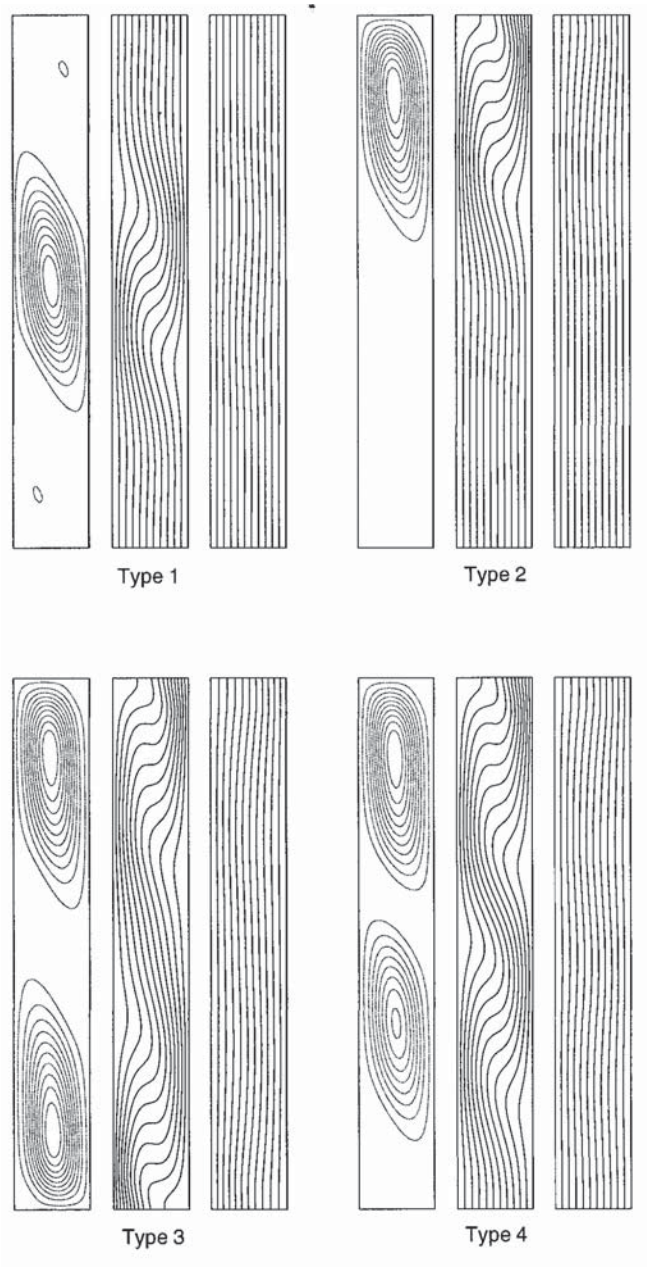

FIG. 13. The multiplicity of subcritical solutions for a cavity with an aspect ratio of $A=7$, all the solutions correspond to $Le=11$, $Ra_T=550$. The dotted lines designate clockwise rotation.

tions show that, in the region of moderate Lewis numbers, $Le<21$, there is the greatest influence of the Lewis number on the onset of the subcritical flow. For large Lewis numbers, $Le>81$, $Ra_{o1}Le$ converges asymptotically to a constant value as Le increases. In the case of the square cavity, this asymptotic value of $Ra_{o1}Le$ is equal to 7200.

ACKNOWLEDGMENT

This work has been carried out with the support of CNES (Center Nationale d'Etudes Spatiales).

[1]R. W. Schmidt, ''Double diffusion in oceanography,'' Annu. Rev. Fluid Mech. **26**, 255 (1994).
[2]W. R. Wilcox, ''Transport phenomena in crystal growth from solution,'' Prog. Crystal Growth Charact. **26**, 153 (1993).
[3]J. S. Turner, ''Multicomponent convection,'' Annu. Rev. Fluid Mech. **17**, 11 (1985).
[4]B. Gebhart, Y. Jaluria, R. L. Mahajan and B. Sammakia, *Buoyancy Induced Flows and Transport* (Hemisphere, Bristol, PA, 1988).
[5]S. A. Thorpe, P. P. Hutt, and R. Soulsby, ''The effect of horizontal gradients on thermohaline convection,'' J. Fluid Mech. **38**, 375 (1969).
[6]J. Tanny and A. B. Tsinober, ''The dynamics and structure of double-diffusive layers in sidewall-heating experiments,'' J. Fluid Mech. **196**, 135 (1988).
[7]C. G. Jeevarag and J. Imberger, ''Experimental study of double-diffusive instability in sidewall heating,'' J. Fluid Mech. **222**, 565 (1991).
[8]S. G. Schladow, E. Thomas, and J. R. Koseff, ''The dynamics of intrusions into a thermohaline stratification,'' J. Fluid Mech. **236**, 127 (1992).
[9]J. E. Hart, ''On side ways diffusive instability,'' J. Fluid Mech. **49**, 279 (1971).
[10]S. Thangam, A. Zebib, and C. F. Chen, ''Transition from shear to sideways diffusive instability in a vertical slot,'' J. Fluid Mech. **112**, 151 (1981).
[11]J. E. Hart, ''Finite amplitude sideways diffusive convection,'' J. Fluid Mech. **59**, 47 (1973).
[12]O. S. Kerr, ''Heating a salinity gradient from vertical sidewall: linear theory,'' J. Fluid Mech. **207**, 323 (1989).
[13]O. S. Kerr, ''Heating a salinity gradient from vertical sidewall: Nonlinear theory,'' J. Fluid Mech. **217**, 520 (1990).
[14]N. Tsitverblit and E. Kit, ''The multiplicity of steady flows in confined double diffusive convection with lateral heating,'' Phys. Fluids **5**, 1062 (1992).
[15]N. Tsitverblit, ''Bifurcation phenomena in confined thermosolutal convection with lateral heating: Commencement of double-diffusive regime,'' Phys. Fluids **7**, 718 (1995).
[16]Y. Kamotani, L. W. Wang, S. Ostrach, and H. D. Jiang, ''Experimental study of natural convection in shallow enclosures with horizontal temperature and concentration gradients,'' Int. J. Heat Mass Transfer **28**, 165 (1985).
[17]S. Ostrach, H. D. Jiang, and Y. Kamotani, ''Thermosolutal convection in shallow enclosures,'' Proceedings of the ASME/JSME Thermal Engineering Joint Conference 158, 1987 (unpublished).
[18]H. D. Jiang, S. Ostrach, and Y. Kamotani, ''Thermosolutal convection with opposed buoyancy forces in shallow enclosures,'' ASME HTD **28**, 165 (1988).
[19]H. D. Jiang, S. Ostrach, and Y. Kamotani, ''Unsteady thermosolutal transport phenomena due to opposed buoyancy forces in shallow enclosures,'' J. Heat Transfer **113**, 135 (1991).
[20]J. Lee, M. T. Hyun, and K. W. Kim, ''Natural convection in confined fluids with combined horizontal temperature and concentration gradients,'' Int. J. Heat Mass Transfer **31**, 1969 (1988).
[21]H. Han and T. H. Kuehn, ''Double diffusive natural convection in a vertical rectangular enclosure: I. Experimental study,'' Int. J. Heat Mass Transfer **34**, 449, (1991).
[22]J. A. Weaver and R. Viskanta, ''Natural convection in binary gases due to horizontal thermal and solutal gradients,'' J. Heat Mass Transfer **113**, 141 (1991).
[23]C. Béghein F. Haghighat, and F. Allard, ''Numerical study of double-diffusive natural convection in a square cavity,'' Int J. Heat Mass Transfer **35**, 833 (1992).
[24]R. L. Mahajan and D. Angirasa, ''Combined heat and mass transfer by natural convection with opposing buoyancies,'' J. Heat Transfer **115**, 606 (1993).
[25]J. M. Hyun and J. W. Lee, ''Double-diffusive convection in rectangle with cooperating horizontal gradients of temperature and concentration,'' Int. J. Heat Mass Transfer **33**, 109 (1990).
[26]J. W. Lee and J. M. Hyun, ''Double-diffusive convection in a rectangle with opposing horizontal gradients of temperature and concentration,'' Int. J. Heat Mass Transfer **33**, 1619 (1990).
[27]H. Han and T. H. Kuehn, ''Double diffusive natural convection in a vertical rectangular enclosure: II. Numerical study,'' Int. J. Heat Mass Transfer **34**, 461 (1991).
[28]R. Bennacer and D. Gobin, ''Cooperating thermosolutal convection in enclosures—I, scale analysis and mass transfer,'' Int. J. Heat Mass Transfer **39**, 2671 (1996).
[29]D. Gobin and R. Bennacer, ''Cooperating thermosolutal convection in enclosures—II, heat transfer and flow structure,'' Int. J. Heat Mass Transfer **39**, 2683 (1996).
[30]T. L. Bergman and M. T. Hyun, ''Simulation of two dimensional thermosolutal convection in liquid metals induced by horizontal temperature and species gradients,'' Int. J. Heat Mass Transfer **39**, 2883 (1996).
[31]R. Krichnan, ''A numerical study of the instability of double diffusive convection in a square enclosure with a horizontal temperature and concentration gradients,'' *ASME National Heat Transfer Conference, Philadelphia 1989* (ASME, New York, 1989), p. 357.
[32]D. Gobin and R. Bennacer, ''Double diffusion in a vertical fluid layer: Onset of the convective regime,'' Phys. Fluids **6**, 59 (1994).
[33]R. G. Drazin and W. H. Reid, *Hydrodynamic Stability* (Cambridge University, Cambridge, England, 1981).
[34]A. Batoul, H. Khallouf and G. Labrosse, ''Une méthode de résolution directe (pseudo-spectrale) du problème de Stokes 2D/3D instationnaire. Application à la cavité entraînée carrée,'' C.R.Acad. Sci. Paris **319**, série II, 1455 (1994).
[35]H. Khallouf, Thèse de doctorat, Univérsité Paul Sabatier, 1995.